Journal of Power Sources 195 (2010) 4356–4364

Contents lists available at ScienceDirect

Journal of Power Sources

journal homepage: www.elsevier.com/locate/jpowsour

Physicochemical, spectroscopic and electrochemical characterization of magnesium ion-conducting, room temperature, ternary molten electrolytes

N.S. Venkata Narayanan, B.V. Ashok Raj, S. Sampath*

Department of Inorganic and Physical Chemistry, Indian Institute of Science, Bangalore 560012, India

ARTICLE INFO

Article history:
Received 14 September 2009
Received in revised form
17 November 2009
Accepted 3 January 2010
Available online 4 February 2010

Keywords:
Room temperature molten electrolyte
Acetamide-based eutectics
Magnesium ion-conductivity
Magnesium rechargeable battery

ABSTRACT

Room temperature, magnesium ion-conducting molten electrolytes are prepared using a combination of acetamide, urea and magnesium triflate or magnesium perchlorate. The molten liquids show high ionic conductivity, of the order of mS cm^{-1} at 298 K. Vibrational spectroscopic studies based on triflate/perchlorate bands reveal that the free ion concentration is higher than that of ion-pairs and aggregates in the melt. Electrochemical reversibility of magnesium deposition and dissolution is demonstrated using cyclic voltammetry and impedance studies. The transport number of Mg^{2+} ion determined by means of a combination of d.c. and a.c. techniques is ~0.40. Preliminary studies on the battery characteristics reveal good capacity for the magnesium rechargeable cell and open up the possibility of using this unique class of acetamide-based room temperature molten electrolytes in secondary magnesium batteries.

1. Introduction

Room-temperature molten ionic liquids are proposed and projected to be good alternates for volatile and harmful organic compounds. They are useful in various areas of application that range from synthesis [1], catalysis [2], extraction [3] and electrochemistry [4] to energy storage [5]. Molten electrolytes have certain unique characteristics such as low vapour pressure, reasonably high ionic conductivity, high thermal stability and a wide electrochemical window. These characteristics, together with environmental friendliness, make them ideal candidates to carry out certain reactions that are otherwise difficult in aqueous and organic media. One such reaction is the Mg dissolution and deposition process that is essential for the development of rechargeable Mg batteries. These batteries have a high power density but have received relatively less attention than their lithium-based counterparts. Mg-based batteries have several advantages such as high charge density (low equivalence weight), high natural abundance of component materials, easy to dispose, and safe to use and handle in ambient atmosphere unlike Li-based systems.

Even though primary batteries based on Mg have been developed way back in 1950s [6], rechargeable version are not yet well-developed and commercialized. There are number of issues and challenges that need to be addressed, namely: (1) the need for a suitable cathode material with appropriate structure and stability for insertion and de-insertion of Mg^{2+} ions over an appreciable number of cycles with reasonable capacity; (2) the need for Mg^{2+} ion-containing electrolytes with high ionic conductivity for reversible deposition of magnesium; (3) the need to develop a strategy to overcome, or minimize, the formation of a passivating layer on the Mg electrode that might compromise the performance of the rechargeable batteries. The present study addresses the second issue, i.e., the development of a suitable Mg ion-conducting electrolyte.

The electrochemistry of magnesium in an aqueous medium suffers from a high overpotential associated with the deposition of metallic magnesium as well as the formation of passivating layers on the Mg negative electrode [7]. Hence, the focus is mainly on the non-aqueous electrochemistry of magnesium [8–10]. Gregory et al. [10] proposed several organo-magnesium compounds and magnesium organoborates dissolved in THF as electrolytes for magnesium rechargeable battery applications. Aurbach et al. [11–13] proposed electrolytes based on magnesium organohaloaluminate salts in THF or polyethers of the glyme family. The addition of LiCl or tetra butylammonium chloride [14] has been shown to improve the accessible electrochemical window. Various electrolytes based on phenyl magnesium chloride and aluminium chlorides that undergo Lewis acid–base reaction in ethereal solvents have been reported by the same group [15].

Gel or solid-polymer electrolytes for rechargeable magnesium batteries are attractive in terms of ease of fabrication, handling and use. There are several reports [16–21] on the use of solid-polymer and gel-polymer electrolytes with polymeric net-

* Corresponding author. Tel.: +91 80 2293 3315; fax: +91 80 2360 1552.
E-mail addresses: sampath@ipc.iisc.ernet.in, sampath2562@gmail.com (S. Sampath).

0378-7753/$ – see front matter © 2010 Elsevier B.V. All rights reserved.
doi:10.1016/j.jpowsour.2010.01.070

works based on poly(methylmethacrylate), polyacrylonitrile or poly(vinylidinefluoride) and organic solvents such ethylene carbonate and propylene carbonate containing magnesium salts. The gel electrolytes have been reported to show good reversibility for the magnesium deposition–dissolution process. On the other hand, gel-polymer and solid-polymer electrolytes suffer from low ionic conductivity under ambient conditions that is mainly due to the poor solubility of magnesium salts. High-temperature molten salt electrolytes such as molten $MgCl_2$ [22], $MgCl_2$ and NaCl [23], MgF_2 and $MgCl_2$ [24], a mixture of chlorides of Ca and Na [25] and a mixture of chlorides of Ca, Na, K and Mg [26] show reversible electrochemical behaviour for the magnesium deposition and dissolution reaction. High-temperature molten salts in batteries are, however, not viable for ambient-temperature applications. By contrast, room-temperature molten electrolytes are attractive but studies are very limited. Towards this direction, 1-n-butyl-3-methylimidazolium tetrafluoroborate [27–29] and N-methyl-N-propylpiperidinium bis(trifluoromethylsulfonyl) imide [28,30] with added magnesium triflate have been reported to show reversible Mg redox processes. Hence, there is a need to find room-temperature electrolytes with reasonably high ionic conductivity for magnesium.

Acetamide and its eutectics form room-temperature molten solvents [31] that have interesting physicochemical properties. The solvent properties of molten acetamide are similar to those of water, with a high dielectric constant of 60 at 353 K. Its acid–base properties are also similar to those of water and it can also dissolve a variety of organic and inorganic compounds. The discovery of acetamide-based molten solvents dates back to Soviet agricultural scientists [32] who stumbled upon the amide-based eutectics during the search for liquid fertilizers. Herein, a new class of room-temperature molten electrolytes with high Mg ionic conductivity, of the order 1 mS cm^{-1} at 298 K is reported. Acetamide has a melting point of 358 K and urea has a melting point of 406 K. Acetamide and urea form a eutectic mixture [31] which is liquid above 328 K. Addition of a third component lowers the melting temperature and the resultant liquids have a tendency to supercool.

The preparation of room-temperature molten electrolytes based on acetamide, urea and magnesium perchlorate or magnesium triflate is reported in the present study. The molten electrolytes good magnesium ion-conducting liquids and are characterized in terms of various physiochemical parameters such as conductivity, surface tension, viscosity and density. Vibrational spectroscopy has been used to identify the presence of ion-pairs and aggregates and is essential to understand the ionic conductivity behaviour. Preliminary studies on battery characteristics have been carried out with γ-MnO_2 as the cathode and Mg as the anode, along with the ternary molten electrolyte developed in the present study.

2. Materials and methods

2.1. Preparation of ternary molten electrolytes

Acetamide and urea were of AR (Analytical reagent) grade and were obtained from SD Fine Chemicals, India. They were dried over molecular sieves for several days prior to use. Magnesium triflate and magnesium perchlorate were purchased from Aldrich, USA, and used as-received. Preparation of the ternary melt was carried out in a closed glass vessel. Acetamide was melted at 358 K and the required amounts of urea and magnesium triflate or magnesium perchlorate were added and stirred until a clear liquid was formed. Subsequently, the molten liquid was cooled to room temperature and stored in inert atmosphere for further use. The composition consisted of 0.57 mole fraction of acetamide, 0.38 mole fraction of urea with 0.05 mole fraction of magnesium triflate and 0.56 mole fraction of acetamide, 0.37 mole fraction of urea, with 0.07 mole fraction of magnesium perchlorate.

2.2. Characterization

Infrared spectroscopy was carried out in the transmittance mode (Perkin Elmer, Spectrum one model FT-IR) with the ternary melt dispersed in KBr. The sample was prepared by mixing a few drops of the electrolyte with KBr and subsequently pressing to form a pellet. The IR spectra were found to be the same when a drop of the melt was placed on a single-crystal Si substrate and used instead of dispersing in KBr. Raman spectroscopy was carried out with a Renishaw model Raman microscope (WiRE model VI.3) that had an incident laser wavelength of 514.5 nm. Differential scanning calorimetry was performed using a differential scanning calorimeter (TA Instruments Q100) in sealed aluminum pans under nitrogen flow at the rate of 5 K min^{-1}. The molten electrolytes were first cooled to 173 K and held at that temperature for 10 min. The samples were then heated at a rate of 5 K min^{-1} up to 473 K. The presence of moisture was avoided by continuously flowing dry nitrogen around the sample compartment, during the experiment. Surface tension measurements were carried out by means of the pendant drop method using a Phoenix 300 SEO surface tension/contact angle analyzer attached to a CCD camera. Measurements at elevated temperature were performed with a hot stage controlled by an external PID controller. The temperature was maintained at ±1 K to the actual value. The data reported is the average of four different measurements. Specific conductivity measurements were carried out using a conductivity cell well (Orion 3 star, Thermoelectron Corporation, USA) with a cell constant of 1.01 cm^{-1}. Constant temperature was achieved with an external water bath at ±1 K. Viscosity measurements at different temperatures were obtained with a theometer (TA Instrument AR-1000-N Rheolyst model).

Electrochemical characterization based on voltammetry and charge–discharge behaviour was undertaken with an electrochemical system (Model, 660A, CHI, USA). Impedance analysis was performed in the frequency range 100 kHz to 0.1 Hz (Model 680 provided with 10A booster, CHI, USA) and a 5 mV peak-peak a.c. signal was used over 0 V d.c. bias. Scanning electron microscopic studies were made with a FEI model SIRION FE-SEM operated at 20 kV. Energy dispersive X-ray analysis (EDAX) at different spots on the sample surface was also carried out to ascertain the elemental composition of the deposited sample. A three-electrode cell was used to characterize the melt with Mg foil as the counter and the reference electrode, and Pt wire as the working electrode. For two electrode cells, both non-blocking and blocking electrode configurations were used with a polypropylene separator containing the melts. Non-blocking, symmetric type cells were fabricated using Mg metal of area 0.8 cm^2 while the blocking interface employed stainless-steel electrodes of area 1 cm^2. Rechargeable batteries were assembled with Mg metal and γ-MnO_2 as the anode and the cathode, respectively, along with a polypropylene separator that contained the ternary melt electrolyte.

3. Results and discussion

The composition used for the preparation of ternary molten electrolyte containing magnesium salt is based on the ratio reported for the molten solvent containing acetamide, urea and ammonium nitrate [31,32] that has been shown to possess good ionic conductivity. The binary eutectic of acetamide and urea forms a liquid at 358 K and subsequent addition of either magnesium perchlorate or magnesium triflate results in

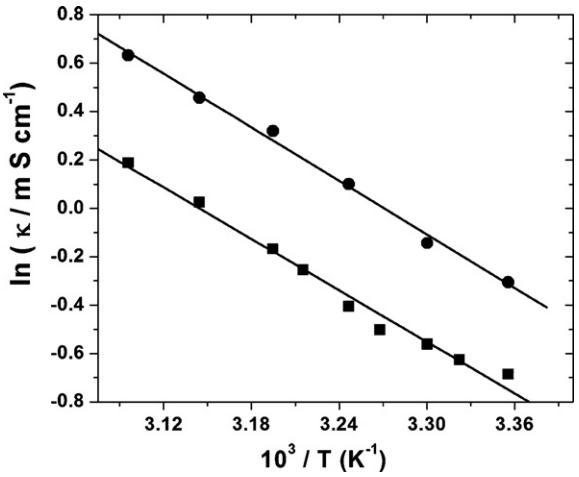

Fig. 1. Arrhenius plots of logarithm of conductivity versus inverse of temperature for magnesium triflate (■) and magnesium perchlorate (●) containing ternary melts.

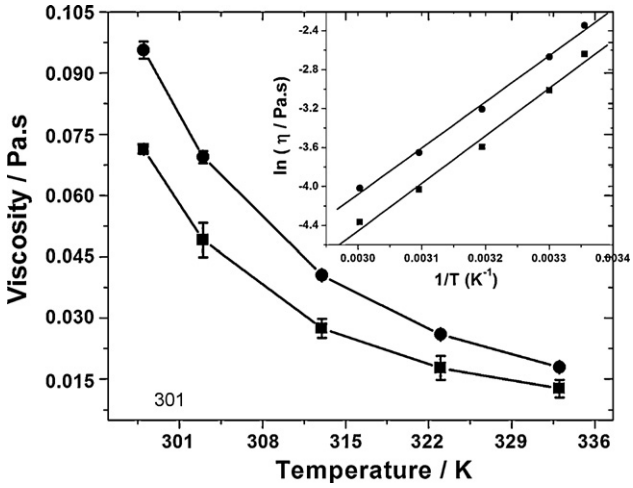

Fig. 2. Viscosity of Mg triflate (■) and Mg perchlorate (●) containing ternary melts as a function of temperature. Inset shows Arrhenius plots of logarithm of viscosity versus inverse of temperature for both melts.

a room-temperature liquid. The composition results in excellent stability of the molten electrolyte over long periods of several weeks to months without any spontaneous nucleation and precipitation.

3.1. Physicochemical characterization

The ionic conductivity of molten electrolytes determines their use in electrochemical applications. The ionic conductivity of a magnesium triflate containing melt at 298 K is found to be 0.5 mS cm^{-1}, whereas a magnesium perchlorate containing melt shows a value of 1 mS cm^{-1} at the same temperature. A eutectic mixture of acetamide and urea has negligible conductivity (less than μS cm^{-1}) at 358 K. Hence, the high conductivity observed with the molten electrolytes is due to the presence of magnesium salts. The ionic conductivity is comparable with, or even higher than, commonly available room-temperature molten liquids. The variation of ionic conductivity as a function of temperature is presented in Fig. 1. The conductivity follows classical Arrhenius behaviour and the activation energy determined for a magnesium triflate containing melt is 29 kJ mol^{-1}, compared with 30 kJ mol^{-1} for a magnesium perchlorate containing melt. It has been reported that the viscosities of molten liquids at a given temperature are generally higher than those of common solvents [4]. Viscosity has direct influence on the ionic conductivity and, consequently, the electrochemical properties. At 298 K, the viscosity of the magnesium triflate containing ternary melt is 71 mPa s and for the melt containing magnesium perchlorate is 96 mPa s. The viscosities at high temperatures are almost equal. The viscosities of the acetamide-based molten liquids are still considerably lower than the values observed for other molten solvents [4,33]. For example, room-temperature ionic liquids such as 1-butyl-3-methyl-imidazolium hexafluorophosphate and 1-butyl-3-methylimidazolium tetrafluoroborate have viscosity of 300 mPa s [33] and 150 mPa s [33], respectively, at 298 K. Plots of viscosity (η) versus temperature are given in Fig. 2. The variation of viscosity as a function of temperature follows Arrhenius behaviour, i.e.,

$$\ln\ \eta = \ln\ \eta_0 + \frac{E_\eta}{RT} \quad (1)$$

where E_η is the activation energy required for viscous flow; T is the temperature in Kelvin; R is gas constant in J K^{-1} mol^{-1}; and η_0 is the pre-exponential factor. The activation energy obtained for the magnesium triflate containing ternary melt is 41.8 kJ mol^{-1} and that for the magnesium perchlorate containing melt is 37.0 kJ mol^{-1}. The density of the two ternary melts is 1.19 g cm^{-3} and is considerably lower than most of the common molten solvents which have densities in the range between 1.2 and 1.50 g cm^{-3} [33].

Various theoretical models have been proposed to account for the behaviour and properties of molecular liquids and molten solvents, for example, the hole theory model [34]. The behaviour of any liquid that has large volume of fusion may be described by this model, which is based on the fact that the liquids consist of holes or cavities of various sizes and shapes that are in dynamic equilibrium. The movement of ions within the solvents depends on the ion to hole radius ratio. In order to have good ionic conduction, the hole size should be larger than, or of the same size as, that of ions present in the melt. Abbott et al. [35] have used the hole theory model to characterize molten solvents that consist of acetamide and zinc chloride/urea and zinc chloride systems. The radius of the hole present in the molten electrolyte can be determined based on surface tension measurements. The surface tension of a molten solvent is related to the hole radius by the following relation [34].

$$4\pi \left\langle r^2 \right\rangle = 3.5\frac{\mathrm{kT}}{\gamma} \quad (2)$$

where γ is the surface tension of the molten solvent in mN m^{-1}; k is the Boltzmann constant; T is the temperature in Kelvin. The surface tension of the magnesium triflate containing melt is 39.0 mN m^{-1} and that of the magnesium perchlorate-based melt is 44.9 mN m^{-1} at 298 K. The low surface tension of the magnesium triflate containing melt compared with the magnesium perchlorate containing melt is in parallel with the viscosity data described earlier. Based on surface tension values, the hole radius of the magnesium perchlorate containing melt is 1.6 Å and that of the magnesium triflate containing melt is 1.7 Å at 298 K. The hole radius observed for acetamide-based melts is higher than that reported for most of the imidazolium based liquids (1.2–1.5 Å), and this results in improved ionic conductivity for the ternary molten electrolytes. The variation of surface tension as a function of temperature is given in Fig. 3. Surface tension values of both melts vary linearly with temperature. According to the principle of independent surface action proposed by Langmuir [36], each part of a molecule possesses a local surface free energy and hence the measured surface tension should correspond to the part of the molecule that is present at the interface. This implies that the surface tension values are determined within a sub-molecular length scale from the free surface. A linear decrease of surface tension as a function of temperature is described by a

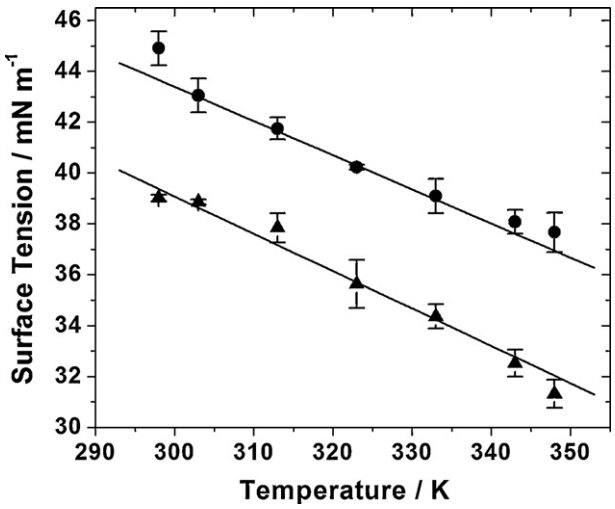

Fig. 3. Surface tension as a function of temperature for Mg triflate (▲) and Mg perchlorate (●) containing ternary melts. Straight lines indicate linear fit of experimental data points.

following relation [37].

$$\gamma(T) = a - bT \quad (3)$$

where intercept 'a' can be identified with the surface excess energy (E_a) and the slope 'b' can be identified with surface excess entropy (S_s). The value of S_s for the triflate containing melt is found to be 0.15 mJ K^{-1} m^{-2} and that for the perchlorate containing melt is 0.13 mJ K^{-1} m^{-2}. The E_a determined for the triflate containing melt is 83.2 mJ m^{-2} and that for the perchlorate containing melt is 83.7 mJ m^{-2}. The values are smaller than that observed for fused salts such as $NaNO_3$ [38] (E_a, 146 mJ m^{-2}), but slightly higher than that observed for 1-methyl-3-pentylimidazolium tetrafluoroborate (67 mJ m^{-2} [39]), 1-methly-3-butlylimdiazolium hexafluorophosphate (69.2 mJ m^{-2} at 336 K [40]) and 1-methyl-3-butylimidazolium tetrafluoroborate (57.6 mJ m^{-2} at 336 K [40]). The E_a of ternary molten electrolytes are slightly higher than the values reported for organic solvents such as benzene (67 mJ m^{-2}) and n-octane (51.1 mJ m^{-2} [38]). The low surface excess energy of the melts compared with fused salts such as $NaNO_3$ implies that interaction energy between ions in the molten solvents is less than that in the case of fused salts but is comparable with organic solvents and dialkylimidazolium-based molten solvents.

Differential scanning calorimetric analysis gives information on the phase transitions and glass transition temperature associated with the molten liquids. The DSC thermograms (supplementary material) reveal glass transition temperatures of 208 and 214 K for the electrolytes containing magnesium triflate and magnesium perchlorate, respectively. One of the remarkable tendencies of

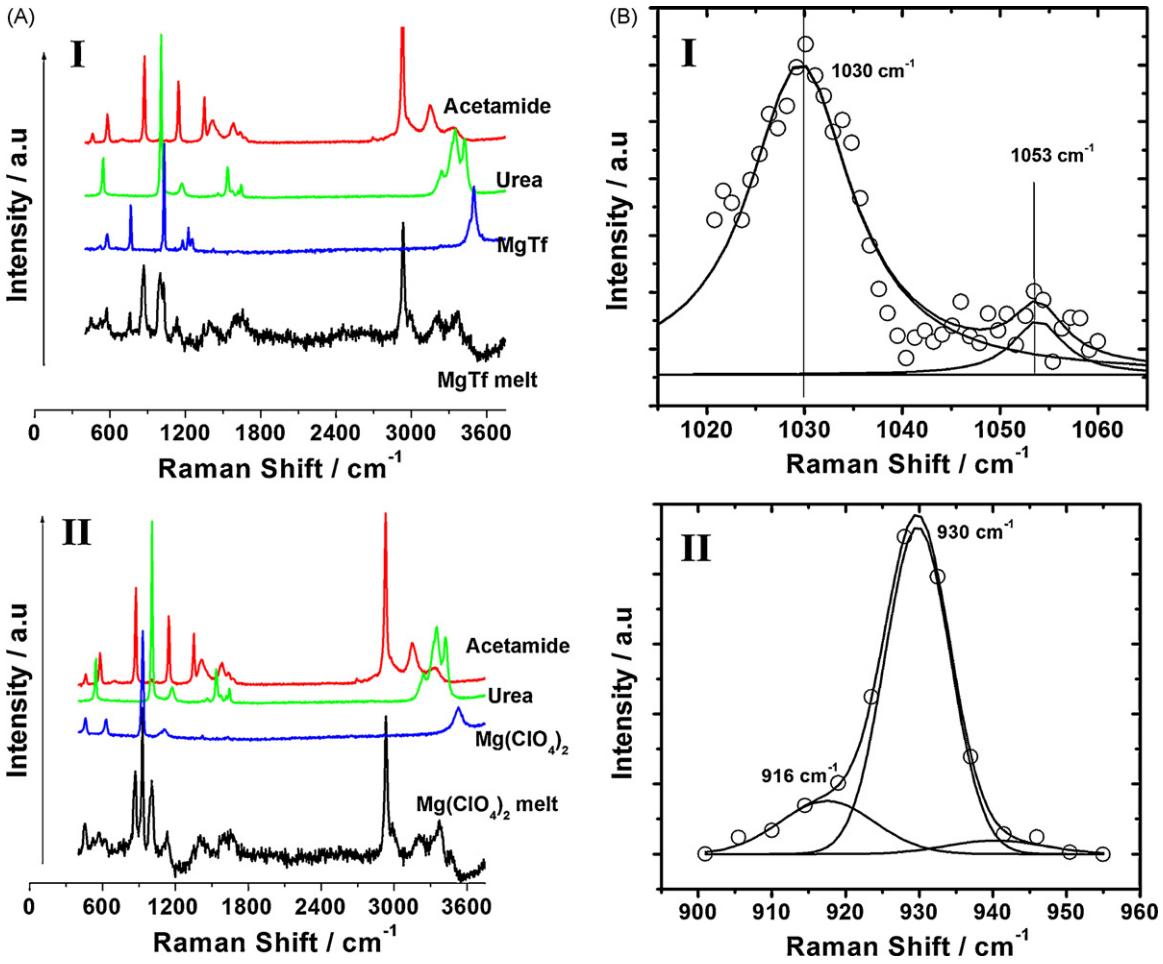

Fig. 4. (A) Raman spectra of (I) magnesium triflate and (II) magnesium perchlorate containing ternary melts. Spectra of individual components, namely, acetamide, urea and magnesium triflate and magnesium perchlorate are also given. Spectra are artificially stacked for clarity. (B) Deconvoluated spectra of (I) triflate (1030 cm^{-1}) and (II) perchlorate (931 cm^{-1}) bands in ternary melts containing magnesium triflate and magnesium perchlorate respectively. Open circles represents actual data points and solid lines are non-linear least-square fits.

acetamide-based molten solvents is their ability to supercool [31] and remain in liquid state for long time without any appearance of crystals. The thermograms do not show the formation of a separate phase after the glass transition temperature is reached. The DSC thermograms are recorded by first cooling the molten liquids at a rate of 5 K min^{-1} until 173 K, followed by heating at the same rate until 473 K. In the case of the ternary melt containing magnesium triflate, a step in the base line is observed around 393 K after the glass transition temperature. The origin of this step is presently not clear. The decomposition of the melt takes place as evidenced by a large endotherm at 463 K. In the case of the ternary melt containing magnesium perchlorate, no such step at 393 K is observed. The decomposition of the melt begins around 423 K as observed by the large endotherm. It is hence possible to use the molten electrolytes up to 383 K without causing any significant decomposition.

3.2. Vibrational spectroscopic characterization

Raman spectroscopy yields information on the nature of ionic species in the electrolyte. The free triflate anion belongs to the point group symmetry, C_{3V}, with the irreducible representation of $5A_1 + A_2 + 6E$. The A_1 and E modes are IR and Raman active. The antisymmetric SO_3 stretching mode [$\nu_a(SO_3)$] that belongs to the representation E is doubly degenerate, whereas the symmetric [$\nu_s(SO_3)$] stretching mode that belongs to A_1 representation is non-degenerate. The Raman spectra of both the melts along with the spectra of individual components are shown in Fig. 4A. In the case of the magnesium triflate containing melt, the region corresponding to the triflate anion gives information on the nature of ion-pair and aggregates present in the molten electrolyte. The band observed at 1031 cm^{-1} corresponds to the symmetric SO_3 stretching [$\nu_s(SO_3)$] of the free triflate anion. The deconvolution (Fig. 4B) gives rise to an additional band at 1053 cm^{-1} which is indicative of ion-pairs/aggregates in the melt. The Raman spectra of the magnesium perchlorate containing melt show the characteristic band for the free perchlorate ion at 931 cm^{-1} along with the bands for ion-pair/aggregates which appear at 916 cm^{-1}. In both cases, the intensities of the bands corresponding to free ions are large and this is an indication of high ionic conductivity. The individual components, namely, acetamide and urea, have characteristic bands corresponding to NH, CN and C=O stretching that appear in the region between 1200 and 1800 cm^{-1}. Acetamide shows NH_2 deformation bands at 1645 and 1636 cm^{-1} whereas urea shows deformation bands at 1645 and 1620 cm^{-1}. The Raman spectrum of the ternary melt gives a broad band in this region with a simultaneous shift in the position of the NH_2 deformation bands to 1657 and 1640 cm^{-1}. The combination of acetamide and urea is expected to result in extensive hydrogen bonding and the addition of magnesium triflate may possibly weaken the extent of hydrogen bonding by interacting with the NH_2 groups present in the base melt. This might result in band broadening with simultaneous shift in the band positions observed for NH_2 deformation modes. Similar shifts in band position, as well as broadening, are observed for the C=O and CN stretching modes. The region between 800 and 1200 cm^{-1} also shows similar features. The strong CN symmetric stretching band at 1008 cm^{-1} for urea broadens in the magnesium triflate containing melt and thereby indicates possible interactions of triflate anion with the individual components of the melt. Thus, based on vibrational spectroscopic characterization, it can be concluded that magnesium triflate/magnesium perchlorate interacts with acetamide and urea. FT-Raman band assignments for individual components and for both ternary melts are provided in the supplementary material (Tables S3 and S4).

The representative FT-IR spectra of both the melts are presented in Fig. 5. Free triflate anion shows an asymmetric stretching

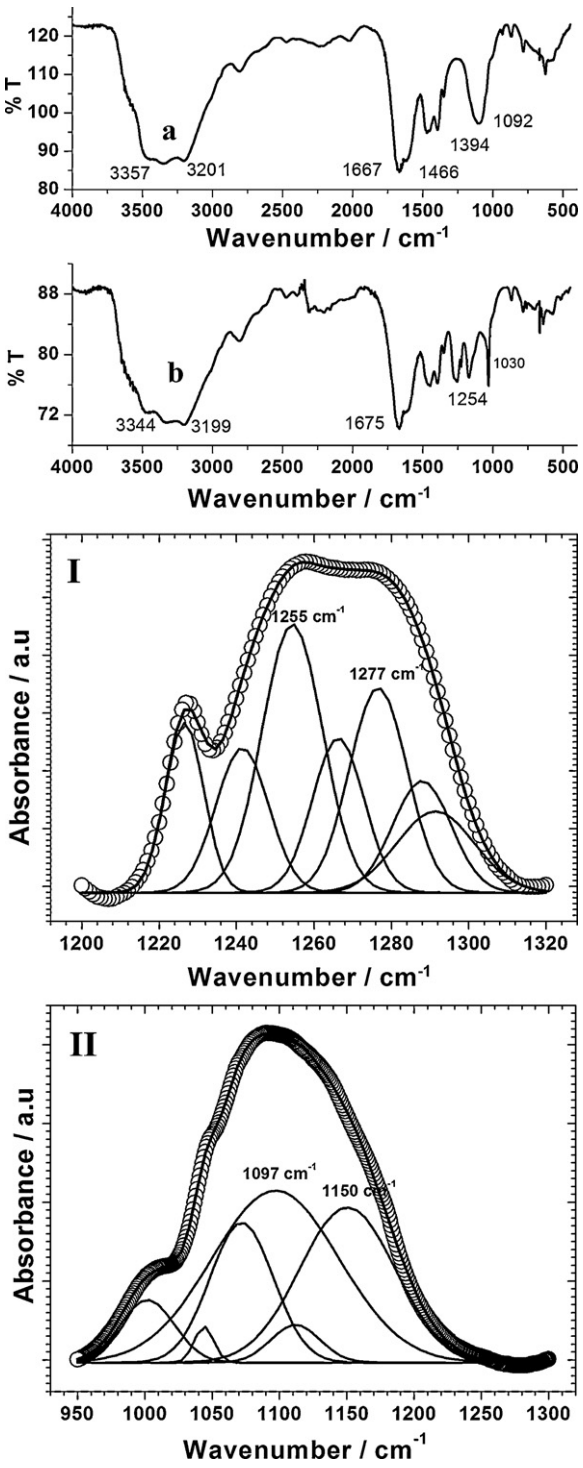

Fig. 5. FT-IR spectra of (a) magnesium perchlorate and (b) magnesium triflate containing ternary melts. Bottom spectra show deconvoluated spectra of triflate ion (I) and perchlorate ion (II) bands showing split of degeneracy. In I and II, open circles represents the actual data points and solid lines are non-linear least-square fits.

mode [$\nu_a(SO_3)$] at 1274 cm^{-1} and the band at 1225 cm^{-1} is due to the symmetric stretching mode of CF_3 [$\nu_s(CF_3)$] [41]. It has been observed that in presence of strongly interacting cations, the asymmetric stretching band [$\nu_a(SO_3)$] splits and gives rise to additional bands at low wave numbers. In the case of magnesium triflate containing ternary melt, the [$\nu_a(SO_3)$] band is observed at 1277 cm^{-1} which corresponds to the presence of free triflate anion. The additional band at 1255 cm^{-1} indicates an interaction of triflate anions

with the Mg^{2+} ion present in the melt. Perchlorate ion has a tetrahedral symmetry with two normal modes of vibration that are IR active [42]. The band corresponding to ν_3 at 1100 cm^{-1} and ν_4 at 624 cm^{-1} are the active modes and are observed at 1097 and at 630 cm^{-1}, respectively. The appearance of additional bands and partial lifting of degeneracy of ν_3 bands with bands at 1150 and 1047 cm^{-1} indicates a strong change in the geometry of the perchlorate anion. FT-IR band assignments for individual components and for both ternary melts are given in the supplementary material (Tables S1 and S2).

3.3. Electrochemical characterization

The redox reaction $Mg \leftrightarrows Mg^{2+} + 2e^-$ needs to be carried out reversibly in order to use the electrode/electrolyte system for any battery application. There are only a few compounds of magnesium that can be used for reversible magnesium deposition and dissolution in non-aqueous media [10–15,43–45]. In the present investigation, the use of magnesium triflate as well as magnesium perchlorate in the ternary melt gives rise to highly conducting molten electrolytes, as described earlier. The cyclic voltammograms with Pt wire as the working electrode and magnesium foil as the counter and reference electrodes (Fig. 6A) are similar to those reported by Aurbach et al. [11] for magnesium organohaloaluminates complexes of the type $MgAlR_nCl_{3-n}$ (where $0 < n < 3$, R = alkyl, aryl). Magnesium deposition and dissolution are clearly observed in both the melts. Scanning electron micrographs (Fig. 6B) as well as elemental analysis (EDAX) show bulk deposition of magnesium on the electrode surface. Cyclic voltammograms of the non-blocking electrode|ternary melt interface as well as the blocking electrode|ternary melt consisting of magnesium perchlorate interface are shown in the inset of Fig. 7. The blocking stainless-steel|electrolyte interface does not show any redox activity in the potential range of −2 to +2 V and the small currents observed are due to changing of the double-layer. The use of a non-blocking magnesium electrode reveals increasing currents leading to peak-shaped voltammograms. This is attributed to the deposition of magnesium from the ternary melt and dissolution of the deposited metal. The impedance plots for blocking and non-blocking interfaces are shown in Fig. 7 over the frequency range from 100 kHz to 5 mHz. The non-blocking interface shows a small semicircle that is related to the resistance associated with the charge-transfer process; the diameter of the semicircle is 102 kΩ cm^2. The Nyquist plot of the blocking interface behaves like a capacitor. Alkali and alkaline earth metals are bound to have surface passivating films to enhance their kinetic stability. It has been suggested that the surface passivating film acts as an interface between the pure metal surface and the electrolyte [46]. There are two layers, one bound to the metal referred to as passivating layer and the second one due to the corrosion/oxidation products over the passivating layer with a porous structure. The passivating layer has been reported to be electronically insulating and hence offers resistance to the charge-transfer process such as the electrodeposition of Mg^{2+} [7]. Solvents such as thionyl chloride in presence of $Mg(AlCl_4)_2$ have been reported [47] to form a SEI at the magnesium|electrolyte interface. The electrochemical reversibility observed in the ternary melt could be due to a combination of breakdown of the passivating layer due to the large overpotential associated with the deposition and contribution of molten electrolyte to interphase formation. It is only speculative and further studies are required to understand the passive layer on magnesium. The experimental Nyquist plot for an Mg symmetrical electrode in presence of ternary eutectic can be fitted by a R (RCQ) (RCQ) (RC) type equivalent-circuit model. The arrangement of the equivalent-circuit model is shown Scheme 1. The maximum frequency used in the impedance measurements and the corresponding capacitance value based on a Cole–Cole plot are 100 kHz and 0.5 μF respectively.

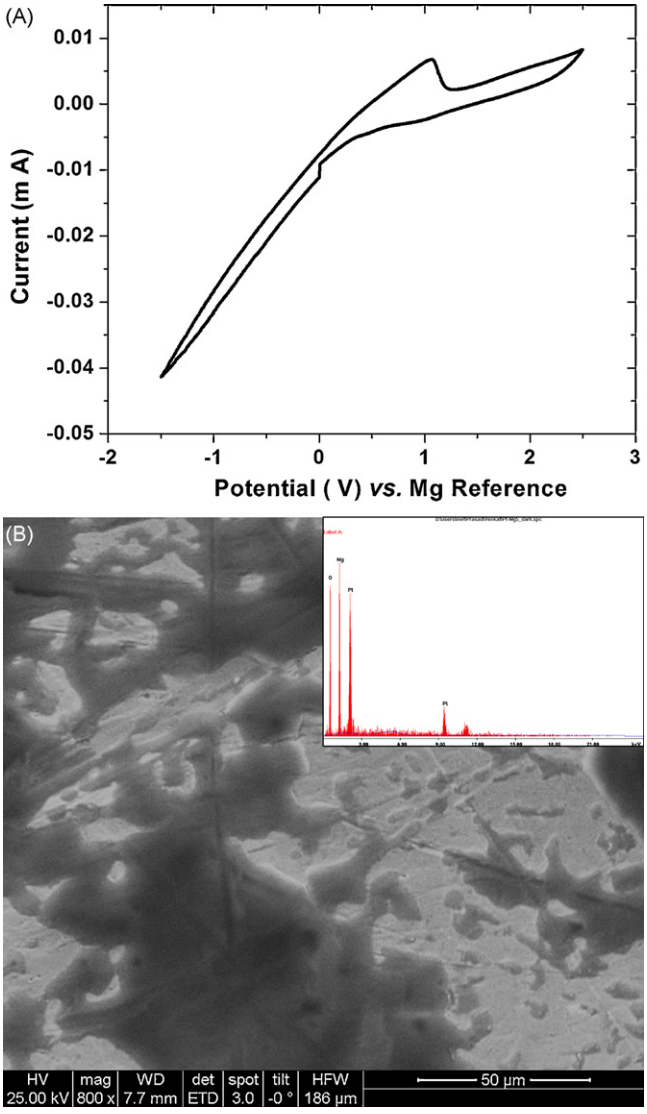

Fig. 6. (A) Cyclic voltammogram obtained on Pt electrode in ternary melt containing magnesium triflate at scan rate of 5 mV s^{-1}. Mg is used as reference and counter electrodes. Geometric area of Pt electrode is 0.18 cm^2. (B) Scanning electron micrograph of Mg deposits on Pt surface obtained from magnesium triflate containing ternary melt. Inset shows EDAX at one specific spot of sample.

The equivalent circuit has two resistance–capacitance combinations together with a constant phase element and one resistance–capacitance combination. This model fits very well with the experimental results (Fig. 8). The physical significance of the first resistance–capacitance combination together with constant phase element may be assigned to the native thin passivating film on the metal electrode, whereas the second resistance–capacitance combination together with constant phase elements is likely to be due to the presence of a porous layer and its interface with the ternary melt. Since the layer is porous, the wettability by the melt depends on the size of the ions present. The third resistance–capacitance combination is assigned to the charge-transfer resistance for the following reaction:

$$Mg^{2+} + 2e^- \rightarrow Mg \quad (4)$$

The value of R_{ct} is 76.85 kΩ cm^2. This low value for the charge-transfer process as compared with the blocking interface (with stainless-steel electrodes) that shows R_{ct} close to 1 MΩ cm^2 and

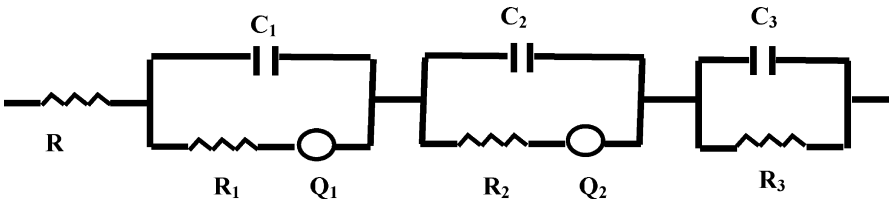

Scheme 1. Equivalent-circuit model used to fit the experimental impedance data of Mg|molten electrolyte|Mg interface.

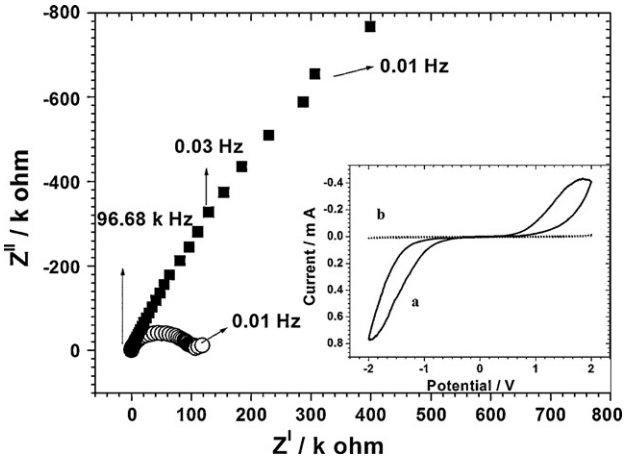

Fig. 7. Nyquist plots for Mg (O) and stainless-steel (■) symmetric electrodes with Mg perchlorate containing ternary melt as electrolyte. Inset shows cyclic voltammograms of (a) Mg (non-blocking electrode, solid lines) and (b) stainless-steel (SS) (blocking electrode, dotted lines) symmetric electrodes using Mg perchlorate containing ternary melt. Scan rate is 5 mV s^{-1}. Area of Mg electrode is 0.8 cm^2 and area of SS is 1 cm^2.

implies the formation of an equilibrium between magnesium metal and the Mg^{2+} ions in the ternary melt. The parameter R is the bulk solution resistance offered by the ternary melt. Further evidence for the formation of the equilibrium is established by calculating the exchange-current density for the redox reaction based on the Butler–Volmer relationship (Eq. (5)), i.e.,

$$i = i_o(\exp^{-2\alpha F\eta_i/RT} - \exp^{2(1-\alpha)F\eta_i/RT}) \quad (5)$$

where i_o is the exchange-current density, α is the transfer coefficient; R is gas constant in J K^{-1} mol^{-1}, T is the temperature in Kelvin η_i is the overpotential. The impedance measurements use a 5 mV a.c. signal over a zero volt d.c. bias and hence Eq. (5) reduces to

$$i_o = \frac{RT}{2FR_{ct}} \quad (6)$$

The exchange-current density is determined by knowing the R_{ct}. An exchange-current density of 0.17 μA cm^{-2} at a temperature of 298 K is observed that establishes the equilibrium between the Mg metal electrode and the Mg^{2+} ions present in the ternary melt. The exchange-current densities reported for gel-polymer electrolytes (GPE) [20–21,48] of poly (vinylidenefluoride) (PVDF) or poly(methylmethacrylate) (PMMA) or poly(acrylonitrile) (PAN) with magnesium triflate are, respectively, 0.2, 0.09 and 0.4 μA cm^{-2}.

The transport number of Mg^{2+} ions has been determined using a combination of a.c. and d.c. techniques [49]. Symmetric non-blocking electrodes of magnesium metal (geometric area, 0.8 cm^2) have been used in presence of the ternary melt. The electrodes are polarized by applying a d.c. bias and impedance measurements are carried out before and after the application of the d.c. pulse in the frequency range, from 100 kHz to 100 mHz (Fig. 9). Initial and steady-state current values are determined from polarization experiments. The transport number is then calculated based on the following expression:

$$t_+ = \frac{I^s(\Delta V - I^oR^o)}{I^o(DV - I^sR^s)} \quad (7)$$

where t_+ is the cation transport number, I^o and I^s are the initial and steady-state currents measured before and after the application of a d.c. bias (ΔV = 0.6 V). R^o and R^s are the initial and steady-state charge-transfer resistance values. The transport number for Mg^{2+} is determined to be 0.42 for a magnesium perchlorate containing melt and 0.39 for a magnesium triflate containing melt, both at 298 K.

Initial attempts have been made to use the ternary melt as an electrolyte in rechargeable magnesium batteries with Mg as the anode and γ-MnO_2 as the cathode with a polypropylene separator containing the ternary melt. The assembled cell is subjected

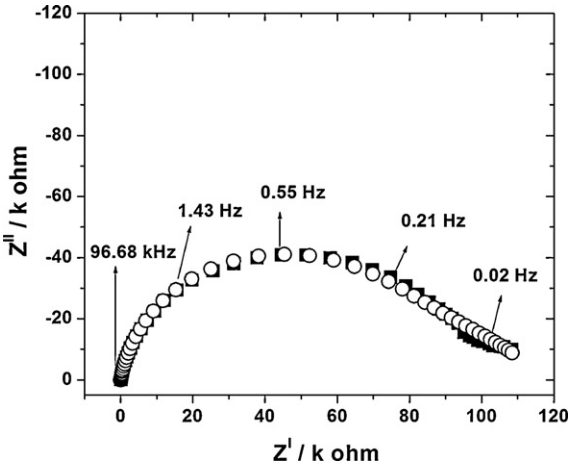

Fig. 8. Experimental and simulated Nyquist plots of Mg metal/ternary melt interface. Closed squares (■) represent experimental data. Simulated data is given as open circles (○).

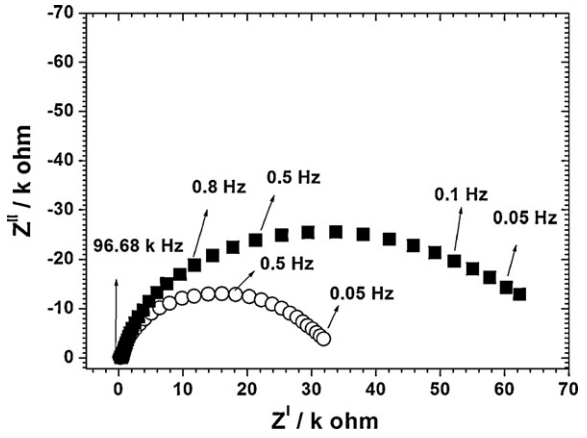

Fig. 9. a.c. impedance plots before (○) and after (■) application of d.c. bias of 0.6 V for magnesium perchlorate containing melt, at 298 K.

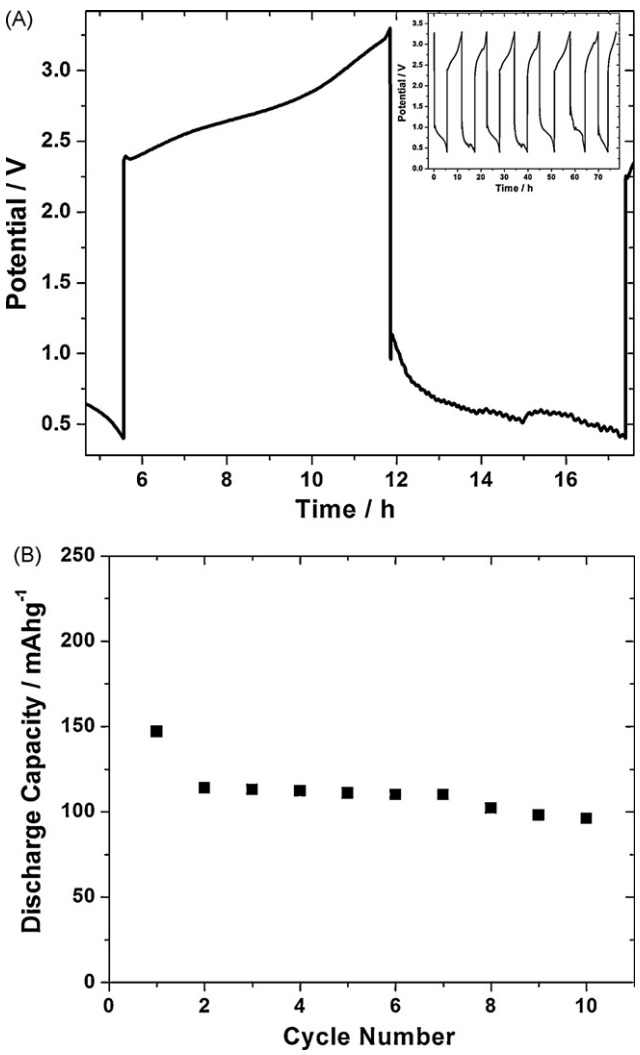

Fig. 10. (A) Charge–discharge cycles (inset shows 8 continuous cycles) for Mg|Mg perchlorate containing ternary melt|γ-MnO_2 cell at a current of 100 μA cm^{-2}. (B) Discharge capacity versus cycle number for Mg|Mg perchlorate containing ternary melt|γ-MnO_2 cell. Mass of active material is 4.5 mg, area of Mg foil is 1 cm^2. Pt mesh (area 1 cm^2) used as current-collector.

to charge–discharge cycles; the cycle is shown in Fig. 10A. The inset of Fig. 10A shows continuous cycles. The potential range is between 3.3 and 0.5 V based on the cyclic voltammetry of the above cell. The capacity for the first cycle is found to be 112 mA h g^{-1} (Fig. 10B) and subsequently gets reduced and stabilizes at around 100 mA h g^{-1} as the cycling progresses. A large iR drop is observed and is to be addressed further by optimizing the cell construction and other parameters. The capacity values are comparable with the discharge capacities obtained using organohaloaluminates based on the glyme family as electrolytes with Mo_6S_8 as the cathode and magnesium as the anode in all solid-state magnesium batteries, as reported by Aurbach et al. [50]. The present studies open up the possibility of using these unique magnesium ion-conducting room-temperature molten electrolytes alternative electrolytes for secondary magnesium-ion batteries. The cell configuration and other parameters are to be further optimized to obtain better performance.

4. Conclusions

Ternary molten electrolytes containing Mg^{2+} ions have been prepared and characterized by various physicochemical and electrochemical techniques. The molten electrolytes show higher ionic conductivity, lower surface tension and relatively lower viscosity than most of the commonly available molten solvents/ionic liquids. The electrochemical studies clearly establish reversible deposition and dissolution of magnesium and preliminary studies on the use of molten solvents as electrolytes for magnesium rechargeable batteries is encouraging. Even though the iR drop observed in the present case is high, further optimization of the cell parameters and suitable choice of insertion cathodes which are not sluggish to Mg^{2+} intercalation may lead to better performance. Nevertheless, this study opens up the possibility of using acetamide-based ternary molten electrolytes for magnesium secondary batteries.

Supplementary material

DSC of the ternary melts; FT-IR and FT-Raman band assignments for individual components and magnesium triflate (MgTf) and $Mg(ClO_4)_2$ containing ternary melts and current versus time transients for $Mg(ClO_4)_2$ and MgTf containing ternary melt.

Acknowledgement

The authors wish to acknowledge DST, CSIR and TIFAC, New Delhi, for financial assistance.

Appendix A. Supplementary data

Supplementary data associated with this article can be found, in the online version, at doi:10.1016/j.jpowsour.2010.01.070.

References

[1] M.A.P. Martins, C.P. Frizzo, D.N. Moreira, N. Zanatta, H.G. Bonacorso, Chem. Rev. 108 (2008) 2015.
[2] J. Dupont, R.F. de Souza, P.A.Z. Suarez, Chem. Rev. 102 (2002) 3667.
[3] J.G. Huddleston, H.D. Willauer, R.P. Swatloski, A.E. Visser, R.D. Rogers, Chem. Commun. (1998) 1765.
[4] M.C. Buzzeo, R.G. Evangs, R.G. Compton, Chem. Phys. Chem. 5 (2004) 1106.
[5] M. Gorlov, L. Kloo, Dalton Trans. (2008) 2655.
[6] C.K. Morehouse, J. Electrochem. Soc. 99 (1952) 187C.
[7] C. Chen, S.J. Splinter, T. Do, N.S. Mclntyre, Surf. Sci. 382 (1997) L652.
[8] N. Amir, Y. Vestfrid, O. Chusid, Y. Gofer, D. Aurbach, J. Power Sources 174 (2007) 1234.
[9] P. Novak, J. Desilvestro, J. Electrochem. Soc. 140 (1993) 140.
[10] T.D. Gregory, R.J. Hoffman, R.C. Winterton, J. Electrochem. Soc. 137 (1990) 775.
[11] D. Aurbach, Z. Lu, A. Schechter, Y. Gofer, H. Gizbar, R. Turgeman, Y. Cohen, M. Moshkovich, E. Levi, Nature 407 (2000) 724.
[12] D. Aurbach, A. Schechter, M. Moshkovich, Y. Cohen, J. Electrochem. Soc. 148 (2001) A1004.
[13] D. Aurbach, H. Gizbar, A. Schechter, O. Chusid, H.F. Gottlieb, Y. Gofer, I. Goldberg, J. Electrochem. Soc. 149 (2002) A115.
[14] Y. Gofer, O. Chusid, H. Gizbar, Y. Viestfrid, H.E. Gottlieb, V. Marks, D. Aurbach, Electrochem. Solid-State Lett. 9 (2006) A257.
[15] O. Mizrahi, N. Amir, E. Pollak, O. Chusid, V. Marks, H. Gottlieb, L. Larush, E. Zinigrad, D. Aurbach, J. Electrochem. Soc. 155 (2008) A103.
[16] N. Yoshimoto, S. Yakushiji, M. Ishikawa, M. Morita, Electrochim. Acta 48 (2003) 2317.
[17] M. Morita, N. Yoshimoto, S. Yakushiji, M. Ishikawa, Electrochem. Solid-State Lett. 4 (2001) A177.
[18] N. Yoshimoto, S. Yakushiji, M. Ishikawa, M. Morita, Solid State Ionics 152–153 (2002) 259.
[19] J.S. Oh, J.M. Ko, D.W. Kim, Electrochim. Acta 50 (2004) 903.
[20] G. Girish kumar, N. Munichandraiah, Electrochim. Acta 47 (2002) 1013.
[21] G. Girish kumar, N. Munichandraiah, Electrochim. Acta 44 (1999) 2663.
[22] A. Kisza, J. Kazmierczak, B. Borresen, G.M. Haarberg, R. Tunold, J. Appl. Electrochem. 25 (1995) 940.
[23] A. Kisza, J. Kazmierczak, B. Borresen, G.M. Haarberg, R. Tunold, J. Electrochem. Soc. 144 (1997) 5.
[24] B. Borresen, G.M. Haarberg, R. Tunold, Electrochim. Acta 42 (1997) 1613.
[25] Y. Castrillejo, A.M. Martinez, R. Pardo, G.M. Haarbergb, Electrochim. Acta 42 (1997) 1869.
[26] A.M. Martınez, B. Børresen, G.M. Haarberg, Y. Castrillejo, R. Tunold, J. Electrochem. Soc. 151 (2004) C508.
[27] Y. NuLi, J. Yang, R. Wu, Electrochem. Commun. 7 (2005) 1105.
[28] P. Wang, Y. NuLi, J. Yang, Z. Feng, Surf. Coat. Technol. 201 (2006) 3783.
[29] Z. Feng, Y. NuLi, J. Wang, J. Yang, J. Electrochem. Soc. 153 (2006) C689.

[30] Y. NuLi, J. Yang, J. Wang, J. Xu, P. Wang, Electrochem. Solid-State Lett. 8 (2005) C166.
[31] R.J. Gale, D.G. Lovering, Molten Salt Techniques, vol. 4, Plenum Press, New York, 1991.
[32] L.S. Bleshchinskaya, K.S. Sulaimankulou, M.D. Davranov, Russ. J. Inorg. Chem. 28 (1983) 607.
[33] A. Lewandowski, M. Galinski, Electrochim. Acta 51 (2006) 5567.
[34] J.O.M. Bockris, A.K.N. Reddy, Modern Electrochemistry, vol. 1, Plenum, New York, 1970.
[35] A.P. Abbott, J.K. Barron, K.S. Ryder, D. Wilson, Chem. Eur. J. 13 (2007) 6495.
[36] I. Langmuir, Phenomena, Atoms and Molecules, Philosophical Library, New York, 1950, p. 72.
[37] J. Lyklema, Fundamentals of Interface and Colloid Science, vol. III, Academic Press, London, UK, 2000.
[38] A.W. Adamson, Physical Chemistry of Surfaces, third ed., Wiley, New York, 1976.
[39] J.Z. Yang, J. Tong, J.B. Li, J.G. Li, J. Tong, J. Colloid Interface Sci. 313 (2007) 374.
[40] G. Law, P.R. Watson, Langmuir 17 (2001) 6138.
[41] A.G. Bishop, D.R. MacFarlane, D. McNanghton, M. Forsyth, J. Phys. Chem. 100 (1996) 2237.
[42] M. Chabanel, D. Legoff, K. Touaj, J. Chem. Soc., Faraday. Trans. 92 (1996) 4199.
[43] C. Liebenow, J. Appl. Electrochem. 27 (1997) 221.
[44] R. Novak, R. Imhof, O. Haas, Electrochim. Acta 45 (1999) 351.
[45] L.P. Lossius, F. Emmenegger, Electrochim. Acta 41 (1996) 445.
[46] E. Peled, in: J.P. Gabano (Ed.), Lithiam Batteries, Academic Press, London, 1983, p. 43.
[47] A. Meitav, E. Peled, J. Electrochem. Soc. 128 (1981) 825.
[48] G. Girish kumar, N. Munichandraiah, J. Power Sources 102 (2001) 46.
[49] J. Evans, C.A. Vincent, P.G. Bruce, Polymer 28 (1987) 2324.
[50] O. Chusid, Y. Gofer, H. Gizbar, Y. Vestfrid, E. Levi, D. Aurbach, I. Riech, Adv. Mater. 15 (2003) 627.